

Prospects of Using the Laser-Induced Temperature Jump Techniques for Characterisation of Electrochemical Systems

Xing Ding⁺,^[a] Theophilus Kobina Sarpey⁺,^[a] Shujin Hou,^[a, b] Batyr Garlyyev,^[a] Weijin Li,^[b, c] Roland A. Fischer,^{*[b, c]} and Aliaksandr S. Bandarenka^{*[a, b]}

Understanding the processes, phenomena, and mechanisms occurring at the electrode/electrolyte interface is a prerequisite and significant for optimizing electrochemical systems. To this end, the advent of sub-microsecond laser pulses has paved the way and eased the investigations of the electrochemical interface (e.g., electric double layer), which hitherto is difficult. The laser-induced current transient (LICT) and laser-induced potential transient (LIPT) techniques have proven to be valuable and unique tools for measuring key parameters of the electrified interface, such as the potential of maximum entropy (PME) and the potential of zero charge (PZC). Herein, we present a summary of studies performed in recent years using laser-

induced temperature jump techniques. The relation between the PME/PZC and the electrocatalytic properties of various electrochemical interfaces are particularly highlighted. Special attention is given to its applications in investigating different systems and analyzing the influence of the electrolyte components, electrode composition and structure on the PME/PZC and various electrochemical processes. Moreover, possible applications of the LICT/LIPT techniques to investigate the interfacial properties of a myriad of materials, including surface-mounted metal-organic frameworks and metal oxides, are elaborated.

1. Introduction

A fundamental understanding of the various electrochemical processes taking place at the interface between the electrode and electrolyte is of crucial importance for several renewable energy provision systems. The often-applied solvent in most electrolytes is water. The interfacial water plays a pivotal role in electrochemical processes and often determines the rate of charge and mass transfer.^[1] Therefore, the investigation of the interfacial water layer structure is necessary to optimize the studied systems.

A key parameter in the description of the electrochemical interface is the potential of zero charge (PZC).^[2] It can be defined as the potential at which the excess charge equals zero on the electrode's surface. This simple definition has, however, a specific shortcoming. Particularly, the evaluation of this

parameter in more complex systems characterized by adsorption processes at the electrified interface is problematic. As such, two types of PZCs have been introduced to circumvent this issue: the potential of zero free charge (PZFC) and the potential of zero total charge (PZTC).^[3] As the names suggest, the PZFC is a type of PZC at which the excess free electronic charge density at the electrode surface is zero. In turn, the PZTC is a potential at which the sum of the free, electronic net charge density and the charge density transferred in adsorption (Faradaic) processes equals zero. Despite the clear difference between the PZFC and PZTC, the two parameters are the same in processes and/or materials that do not exhibit specific adsorption. Under these conditions, one can safely access the values of the PZFC *via* the determination of the PZTC.^[4] Moreover, another essential parameter, the potential of maximum entropy (PME), is closely related to the PZFC.^[5] It is commonly defined as the potential at which the entropy of the double layer formation maximizes. The introduction of the PME is particularly useful when assessing the "stiffness" of the water layer structure at the interface.^[1b] When approaching the PME, the degree of order of the interfacial water molecules decreases. Consequently, the charge and mass transfer through the electric double layer (EDL) should proceed much more easily. In contrast, at potentials far from the PME, the interfacial water layer structure is more rigid, and this slows down the transfer of charge and mass through the EDL. Therefore, the determination of the PME is significant to understanding the processes taking place at the interface.


The PZC can be measured by the electrocapillary method, capacitance method, CO charge displacement, N₂O reduction and, so on.^[6] However, the application of these methods is limited for various specific conditions. The capacitance method can only be used for dilute solutions and in the absence of


[a] X. Ding,⁺ T. K. Sarpey,⁺ S. Hou, Dr. B. Garlyyev, Prof. Dr. A. S. Bandarenka
Physics of Energy Conversion and Storage
Technical University of Munich
James-Franck-Straße 1, 85748 Garching b. München, Germany
E-mail: bandarenka@ph.tum.de

[b] S. Hou, Dr. W. Li, Prof. R. A. Fischer, Prof. Dr. A. S. Bandarenka
Catalysis Research Center TUM
Technical University of Munich
Ernst-Otto-Fischer-Straße 1, 85748 Garching b. München, Germany
E-mail: roland.fischer@tum.de

[c] Dr. W. Li, Prof. R. A. Fischer
Department of Chemistry
Technical University of Munich
Lichtenbergstraße 4, 85748 Garching b. München, Germany

[⁺] These authors contributed equally to this work.

 An invited contribution to the Wolfgang Schuhmann Festschrift

 © 2021 The Authors. ChemElectroChem published by Wiley-VCH GmbH. This is an open access article under the terms of the Creative Commons Attribution License, which permits use, distribution and reproduction in any medium, provided the original work is properly cited.

specific adsorption. The CO charge displacement method cannot be applied at high anodic potentials to avoid CO oxidation, while the N₂O reduction method is limited for the interfacial structure, which is sensitive to the N₂O reduction reaction. It must be emphasized that the N₂O reduction method helps to characterize distinctively between local PZTCs present in a particular sample.^[6] Based on the aforementioned limitations, there is a compelling need to elaborate more versatile techniques. One of such approaches is the laser-induced temperature jump method. A short description of the techniques will be discussed in Section 2.

This short review highlights some recent works that have utilized the LICT/LIPT techniques to investigate the interfacial fundamentals of electrodes in various electrochemical systems. Additionally, an outlook regarding the application of the LICT/LIPT techniques on other non-noble metal-based electrodes, such as metal oxides (e.g., MnO_x) and metal-organic frameworks (MOFs), is discussed.

2. The LICT/LIPT Techniques

The method of probing the electrode/electrolyte interface with short, powerful laser pulses was developed by Benderskii *et al.* in the 1980s.^[7] It utilizes the so-called temperature jump effect to probe the EDL for analyzing the electrochemical systems. Generally, two different methods are applied: the laser-induced potential transient (LIPT) and the laser-induced current transient (LICT) techniques. The former is performed under coulostatic conditions to measure the change of the open-circuit potential. By contrast, the LICIT technique is conducted under potentiostatic conditions to record the current transients (Figure 1a).^[8] In brief, the rapid increase in the electrode/electrolyte interface temperature caused by the laser pulse randomizes the ions and water molecules at the interface. The perturbed electric double layer returns almost rapidly to its initial state since the duration of the applied laser pulse is in the scale of nanosecond (5–10 ns).^[8a] The system's answer is recorded as current transients,^[9] the orientation of which coincides with the sign of the excess charge on the electrode surface. Namely, if the

electrode is negatively charged, negative current transients are observed and *vice versa*. The potential at which the current transient changes its sign can be correlated with the PME (as illustrated in Figure 1b).

3. Applications of LICT/LIPT to Characterise Electrocatalytic Systems

The utilization of the LICT/LIPT techniques has successfully promoted the understanding of interfacial processes, especially in various electrocatalytic systems.^[10] The determination of the PZC/PME gives the information of the double layer order/disorder status. Besides, these parameters are believed to be closely associated with the work function of the metal electrode.^[11]

3.1. PME/PZC Determination of Various Electrode Materials

Interestingly, the PME of Pt(111) in alkaline media was found to be located at the onset potential of the OH-adsorption.^[12] Recently, Sebastián-Pascual *et al.* also demonstrated that the location of the PME was related to the onset potential of the OH-adsorption on both Cu(111) and Cu(100) in 0.1 M NaOH solutions.^[13] Similar results were observed for Cu(111) at the same pH level in our recent work.^[8a] The PME of Cu(111) portrays a linear relationship with the electrolyte pH on the standard hydrogen electrode (SHE) scale. However, the decrease in the electrolyte pH shifts the PME towards the potential within the OH-adsorption region. Moreover, combining with electrochemical scanning tunneling microscopy imaging, it was found that the Cu(111) surface slowly starts to restructure at the PME in the electrolytes at pH = 11 and pH = 13. It should be noted that the pH dependency of the PME varies for the same electrode material with different surface structures.^[11] Besides using noble metal electrodes for the laser-induced temperature jump measurements, the PZC of Mn₂O₃ was also successfully investigated.^[14] The PZC, which is closely related to the PME,

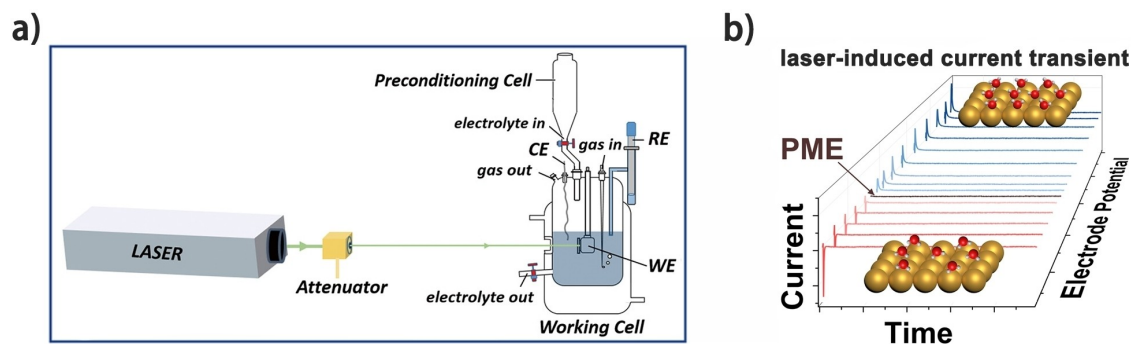


Figure 1. (a) Schematic illustration for the application of the laser-induced temperature jump technique. WE, RE, and CE correspond to working, reference, and counter electrode, respectively. (b) Typical current transients recorded during the laser measurement at various electrochemical potentials via the LICIT. The potential at which the current transient changes its sign corresponds to the PME. (a, b) Reproduced with permission from Ref. [8b]. Copyright (2021) Wiley-VCH.

was located at 1.09 V vs RHE, thus, supporting the notion that Mn_2O_3 should catalyze the oxygen reduction reaction (ORR) well since the obtained PZC is quite close to the thermodynamic equilibrium potential of the ORR. This work demystified and further confirmed the reasons for the good ORR performance of Mn_2O_3 in this kind of electrolytes. Hence, investigating the actual EDL status obtained *via* illuminating the electrode with short laser pulses presents a leeway to investigating other metal oxide materials by employing the LICT/LIPT techniques.

3.2. Effects of Electrode Composition and Structure on the PME/PZC

Due to their great stability, noble metal-based catalysts are used in various electrocatalytic systems.^[15] However, the performance of these metals in electrocatalysis still needs to be improved. To enhance the electrocatalytic performance of the electrodes, one can incorporate certain facets or defects to change the electrode surface structure or create alloys to change the electrode surface composition.^[16] It is believed that this can finally increase the number of active sites at the electrode surface and improve the electrode activity. Thus, tuning the electrode composition and structure changes the performance of the electrode. However, change(s) in the properties of the EDL should also be considered. For instance, Pt single crystals show good performance for the ORR,^[17] while the activity varies for different orientations of the Pt single

crystals.^[12] The difference in activity for different structures of Pt single crystals is due to the difference in the heat of adsorption of intermediates at different active centers and their different abundance.^[16b,18] Interestingly, with the LIPT technique, García-Arárez *et al.* revealed that the locations of the PME for Pt single crystals in acidic solution differ with the surface structure.^[11] Subsequently, Sarabia *et al.* also found a similar influence in the case of alkaline media.^[12] Therefore, the interfacial water layer structure is heavily related to the electrode structure, further affecting the electrode activity. It can be noted that the PME increases in the order of $\text{Pt}(110) < \text{Pt}(100) < \text{Pt}(111)$ in alkaline solutions (see Figure 2a–c), which is in line with the observed results for the ORR.^[19] Namely, the PME for Pt(111) is closer to the thermodynamic equilibrium potential of the ORR. Thus, the interfacial water structure for Pt(111) is more loose and easy to reorganize during the charge and mass transfer through the electric double layer. This could also contribute to the observed situation that Pt(111) presents the best ORR activity among the three crystal orientations.

Although pure noble metals manifest good performance on electrocatalytic activities, modifying the electrode surface with certain transition metal hydroxides enhances the reaction activity.^[20] For instance, adding nickel hydroxides to the Pt(111) surface promotes the rate of the hydrogen evolution reaction (HER).^[21] Traditionally, the effect of the modification on the electrode is believed to correlate with the change in the interaction between the electrode surface and the relevant intermediates.^[22] On that score, Ledezma-Yanez *et al.* demon-

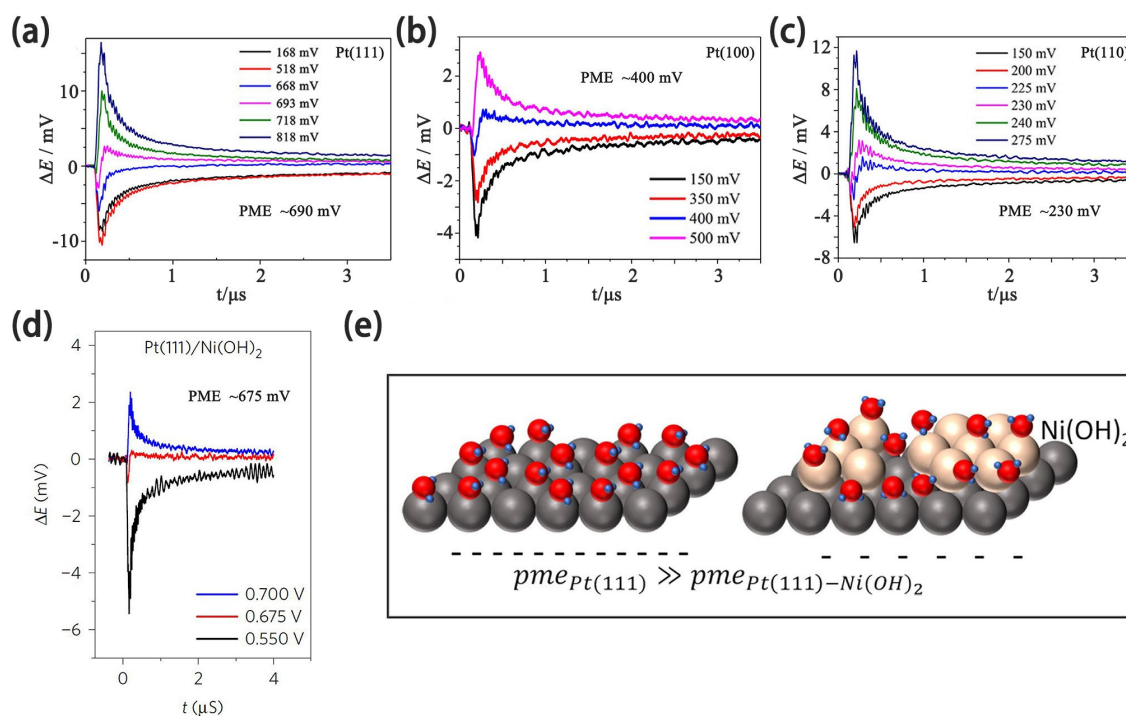


Figure 2. Laser-induced potential transients recorded at different potentials for (a) Pt(111), (b) Pt(100), (c) Pt(110), and (d) Pt(111)/Ni(OH)₂ in 0.1 M NaOH solution. The estimated PMEs are shown. (a–c) Reproduced with permission from Ref. [12]. Copyright (2020) Elsevier. (d) Reproduced with permission from Ref. [1b]. Copyright (2017) Springer Nature. (e) Scheme of the network of water dipoles on Pt(111) and the unstructured network on Pt(111)-Ni(OH)₂. Increasing the nickel coverage shifts the PME to the potentials closer to the thermodynamic equilibrium potential of the HER. Reproduced with permission from Ref. [23]. Copyright (2018) American Chemical Society.

strated that adding Ni(OH)₂ shifts the PME closer to the thermodynamic equilibrium potential of the HER by the LIPT experiments (Figure 2d).^[1b] This means the presence of Ni(OH)₂ lowers the order of the interfacial water layer structure at the onset potential of the HER, which promotes the charge transfer and the kinetics of the reaction. Based on this proposal, Sarabia *et al.* used the LIPT to study further the influence of the coverage of Ni(OH)₂ on Pt(111) on the HER.^[23a] They observed that increasing the Ni(OH)₂ coverage moves the PME to the potential where the HER takes place (Figure 2e). Again, this decreases the order of the electric double layer structure at the potential of the HER and improves the HER activity. Extending the studies on Cu(111), Auer *et al.* recently modified the surface of pristine Cu(111) with 0.1 and 0.2 monolayers (ML) of Ni(OH)₂.^[23b] They reported a non-linear activity behavior when the Ni(OH)₂ coverage was increased, a deviation from the earlier study conducted on Pt(111) surface.^[23a] Further probing using electrochemical scanning tunneling microscopy and the laser-induced temperature jump technique revealed that only the Cu(111) with 0.2 ML of Ni(OH)₂ exhibited high water layer structure disorder at the interface. This observation of the PME was noticed close to the thermodynamic equilibrium potential of the HER and was attributed to reaching the peak of surface roughness while increasing the monolayers of nickel hydroxide on the Cu(111) surface. This therefore induced an increase in disorder of the interfacial water layer structure.

3.3. Effect of Electrolyte Composition on the PME/PZC

In the past decades, most studies have focused on the compositional and structural modification of electrode materials to optimize electrocatalytic systems. Nevertheless, the role of electrolytes is gradually considered valuable.^[24] For instance, it has been widely reported that the electrolyte pH can drastically influence the rate of the HER.^[25] Several hypotheses have been developed to address this issue.^[26] Climent *et al.* discovered that the PME value for Au changes upon variation of the electrolyte pH by using the LIPT technique.^[10d] Similarly, comparable observations were made using Pt as the electrode material and varying the electrolyte pH.^[27] Besides, Martínez-Hincapié *et al.*

demonstrated that there is a variation in pH dependences for the PMEs of Pt(111), Pt(100), and Pt(110) electrodes (Figure 3a).^[28] This finding clarifies the fact that PMEs of different crystallographic orientations of the same electrode might not necessarily show the same behavior with varying electrolyte pH. Ganassin *et al.* also observed the pH dependence of the PME for Ir(111) in acidic media (Figure 3b).^[29] However, hydrogen and specific anion adsorption effect should be considered in the cases which occur on more electroactive materials (Pt and Ir). Because, in the double layer region where there is no specific adsorption, the PME is supposed to be independent of the electrolyte pH on the SHE scale or shift approximately 59 mV per pH unit on the RHE scale.^[5,11,28] Interestingly, the pH dependence of the HER activity has been correlated to the effect of pH on the location of the PME.^[1b]

Apart from the electrolyte pH, the presence of alkali metal cations can also drastically alter the electrocatalytic activity of the electrodes. Their influence on the electrode processes has been investigated in some previous works.^[24b,30] Particularly, Strmcnik *et al.* demonstrated that the activities towards the ORR and hydrogen oxidation reaction on Pt linearly correlate with the hydration energies of the corresponding alkali metal cations.^[24c] Besides, the pH influence can be considerably different in the presence of alkali metal cations. In our recent work, polycrystalline Au in Ar- and O₂-saturated 0.5 M Na₂SO₄ or K₂SO₄ solution was examined using the LICT technique.^[8b] As shown in Figure 3c, it was found that the PME shifts towards more positive potentials as a result of increasing the electrolyte pH and introducing oxygen. This could be due to the variation in the local pH at the interface. Moreover, the PME difference becomes enormous when the electrolyte pH reaches 6, which means, in this case, the electric double layer structures for Au in Na⁺- and K⁺-containing electrolytes are significantly different. Thus, different electrode processes can be expected in electrolytes containing these two cations. Therefore, the utilization of the LICT/LIPT techniques is believed to help promote the fundamental understanding regarding the electrode processes happening in various electrocatalytic systems.

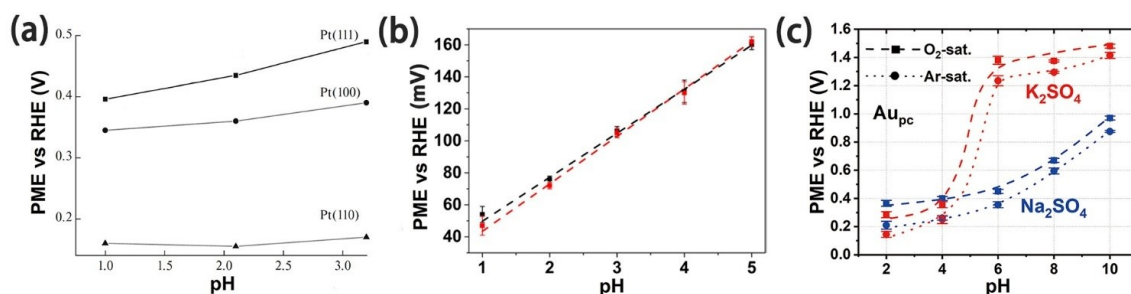


Figure 3. (a) Dependence of the PMEs on the pH for Pt(111), Pt(100), and Pt(110). Reproduced with permission from Ref. [28]. Copyright (2017) Springer Nature. (b) The PMEs plotted as a function of the pH for Ir(111) with (red symbols) and without (black) the thermodiffusion correction. Reproduced with permission from Ref. [29]. Copyright (2017) Springer Nature. (c) The values of the PME for polycrystalline gold in Ar-saturated (dot) and O₂-saturated (dash) 0.5 M Na₂SO₄ (blue) and K₂SO₄ (red) solutions depicted as a function of the electrolyte pH. Reproduced with permission from Ref. [8b]. Copyright (2021) Wiley-VCH.

4. Applications of LICT/LIPT for the Investigation of Aqueous Battery Systems

Batteries have been widely used for renewable energy storage applications.^[31] Especially, aqueous metal-ion batteries have attracted considerable attention owing to their safety, low cost, and wide availability. However, a better understanding of intercalation and de-intercalation processes is still required to improve and optimize the investigated systems.^[32] The LICIT methodology could be a powerful tool to research the field of aqueous metal-ion batteries because the PME of the systems can easily reveal the interfacial charge status during different processes. As the hydration energy of cations and anions could influence the stiffness of the water layer structure at the interface, the resulting PME of the investigated system can be affected by different ions.^[9a,33] For instance, promising electrode material used in aqueous Na-ion batteries, $\text{Na}_2\text{Ni}[\text{Fe}(\text{CN})_6]$, were investigated with the LICIT technique.^[9b] The position of the PME for thin films of $\text{Na}_2\text{Ni}[\text{Fe}(\text{CN})_6]$ in 0.25 M Na_2SO_4 was around -0.13 V vs Ag/AgCl (SSC), while the current transients stayed positive for the case of 0.25 M K_2SO_4 at the same investigated potential region. Interestingly, the obtained results showed that the electrodes were positively charged for both systems during the intercalation processes (Figure 4a, b). Moreover, the LICIT measurements showed the presence of three different PMEs as shown in Figure 4c. This observation could be explained from the different hydration energies hence different ion mobilities occasioned by the different electrolyte composi-

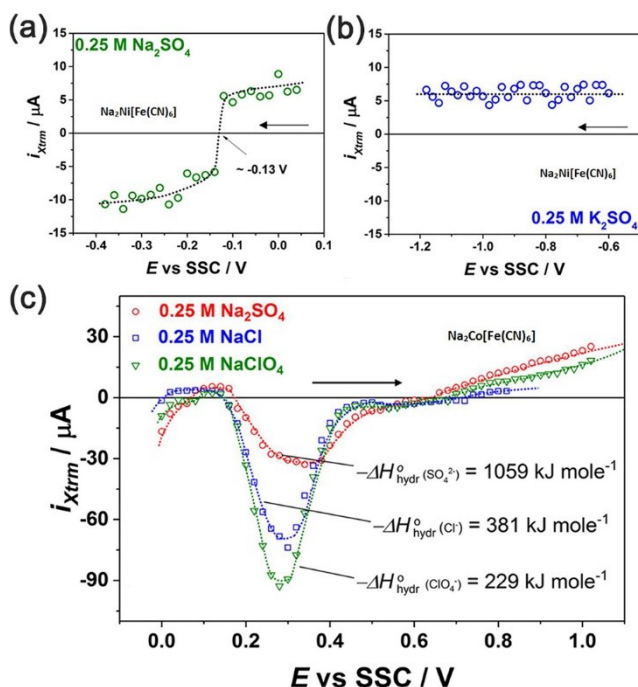


Figure 4. The maximal current transients collected for $\text{Na}_2\text{Ni}[\text{Fe}(\text{CN})_6]$ in (a) 0.25 M Na_2SO_4 , and (b) 0.25 M K_2SO_4 , and for (c) $\text{Na}_2\text{Co}[\text{Fe}(\text{CN})_6]$ in 0.25 M Na_2SO_4 , 0.25 M NaCl , and 0.25 M NaClO_4 . (a, b) Reproduced with permission from Ref. [9b]. Copyright (2017) American Chemical Society. (c) Reproduced with permission from Ref. [9a]. Copyright (2018) American Chemical Society.

tions (Na_2SO_4 , NaCl , and NaClO_4) used for electrodepositing the $\text{Na}_2\text{Co}[\text{Fe}(\text{CN})_6]$ films. It is envisaged that the aforementioned differences influence the interfacial processes, thus, leading to different relaxation times.^[9,33] As mentioned earlier, the PME is associated with the interfacial water layer structure. One can, therefore, correlate the PMEs with the processes taking place at the interface. For this system, the locations of the PMEs are close to the onset potential range of the (de)intercalation of Na^+ , which lies between 0.1 V and 0.9 V vs SSC. The stiffness of the EDL reaches its minimum at the PMEs, which is significant for the (de)intercalation process. These results show that the LICIT/LIPT methods are promising techniques for studying the electrode/electrolyte interfacial phenomena for various electrode materials for aqueous metal-ion batteries.

5. Summary and Perspective

To conclude, we have analyzed recent research articles that employed the LICIT/LIPT techniques to investigate various electrocatalytic and aqueous metal-ion battery systems. From the numerous literature presented, one can vividly establish and confirm the value and uniqueness of these techniques in characterizing the electrode/electrolyte interface as they permit the determination of the PME/PZC of various systems. These parameters help to elucidate the processes occurring at the interface as a function of, for example, electrolyte composition. As a result of its relative simplicity and ease of combining it with other techniques, the LICIT/LIPT methodologies can be applied to various electrocatalytic or aqueous metal-ion battery systems.

As is evident from the works highlighted herein, there is an excellent opportunity to apply LICIT/LIPT techniques to explore other systems containing non-noble metal electrodes, metal oxides, metal-organic frameworks (MOFs), conductive polymers, metal alloys (Figure 5). For instance, our group has recently developed a versatile and facile strategy to synthesize mixed metal hydroxide electrocatalysts derived from surface-mounted

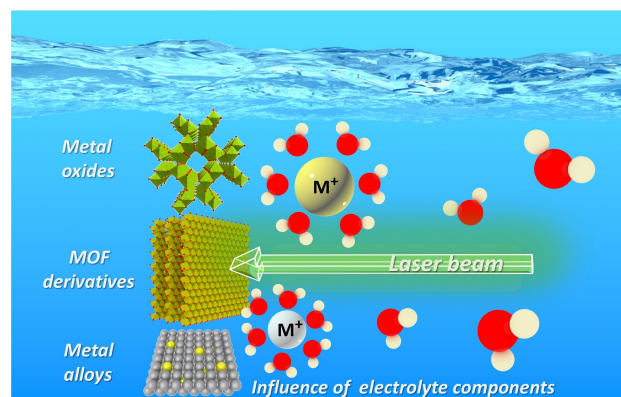


Figure 5. Schematic of the LICIT/LIPT techniques for the investigation of the influence of electrolyte components. Herein, several promising electrocatalyst materials such as metal oxides, MOF derivatives and metal alloys are presented. The LICIT/LIPT techniques provide a unique approach to elucidate the EDL structure-performance relationships in electrochemical systems.

MOFs (SURMOFs) with excellent OER performance in alkaline media.^[34] However, the investigation of the electrolyte effect on MOFs-based systems has rarely been reported since most studies focus on the design of the electrode materials. Therefore, rational electrolyte engineering in MOFs-based systems is required to improve the performance of materials in electrocatalytic systems.

Owing to the presented ability of the LICT/LIPT techniques for improving the fundamental understanding of the electric double layer properties in various simple or complicated electrochemical systems, we envisage these methods can be further applied to other aforementioned systems to investigate the mechanism of the interfacial processes and finally optimize the studied systems.

Acknowledgements

We are grateful for the financial support from Deutsche Forschungsgemeinschaft under Germany's excellence strategy – EXC 2089/1 – 390776260, Germany's excellence cluster “e-conversion”, DFG project BA 5795/5-1 and BA 5795/6-1 and DFG research group 2982 under UNusual anODE (UNODE). X.D. and S. J. H acknowledge financial support from the China Scholarship Council. Open Access funding enabled and organized by Projekt DEAL.

Conflict of Interest

The authors declare no conflict of interest.

Keywords: potential of maximum entropy · laser-induced current/potential transient · electric double layer · electrolyte influence · metal-organic frameworks

- [1] a) J.-J. Velasco-Velez, C. H. Wu, T. A. Pascal, L. F. Wan, J. Guo, D. Prendergast, M. Salmeron, *Science* **2014**, *346*, 831–834; b) I. Ledezma-Yanez, W. D. Z. Wallace, P. Sebastián-Pascual, V. Climent, J. M. Feliu, M. T. Koper, *Nat. Energy* **2017**, *2*, 17031.
- [2] A. S. Shatla, M. Landstorfer, H. Baltruschat, *ChemElectroChem* **2021**, *8*, 1817–1835.
- [3] a) V. Climent, N. García-Araez, E. Herrero, J. M. Feliu, *Russ. J. Electrochem.* **2006**, *42*, 1145–1160; b) A. Frumkin, O. Petrii, *Electrochim. Acta* **1975**, *20*, 347–359.
- [4] T. Pajkossy, D. Kolb, *Electrochim. Commun.* **2003**, *5*, 283–285.
- [5] P. Sebastián, R. Martínez-Hincapié, V. Climent, J. M. Feliu, *Electrochim. Acta* **2017**, *228*, 667–676.
- [6] a) G. Lippmann, Relations entre les phénomènes électriques et capillaires. Gauthier-Villars Paris, France **1875**; b) P. Horsman, B. E. Conway, E. Yeager, *Comprehensive Treatise of Electrochemistry: The Double Layer*, Springer Science & Business Media **2013**; c) S. Trasatti, *J. Electroanal. Chem. Interfacial Electrochem.* **1974**, *54*, 437–441; d) C. D. Silva, G. Cabello, W. A. Christinelli, E. C. Pereira, A. Cuesta, *J. Electroanal. Chem.* **2017**, *800*, 25–31; e) H. Ebert, R. Parsons, G. Ritzoulis, T. VanderNoot, *J. Electroanal. Chem. Interfacial Electrochem.* **1989**, *264*, 181–193; f) V. Climent, G. A. Attard, J. M. Feliu, *J. Electroanal. Chem.* **2002**, *532*, 67–74; g) G. A. Attard, O. Hazzazi, P. B. Wells, V. Climent, E. Herrero, J. M. Feliu, *J. Electroanal. Chem.* **2004**, *568*, 329–342.
- [7] a) V. Benderskii, S. Babenko, A. Krivenko, *J. Electroanal. Chem. Interfacial Electrochem.* **1978**, *86*, 223–225; b) V. Benderskii, G. Velichko, I. Kreitus, *J. Electroanal. Chem. Interfacial Electrochem.* **1984**, *181*, 1–20.
- [8] a) A. Auer, X. Ding, A. S. Bandarenka, J. Kunze-Liebhäuser, *J. Phys. Chem. C* **2021**, *125*, 5020–5028; b) X. Ding, B. Garlyyev, S. Watzele, T. K. Sarpey, A. S. Bandarenka, *Chem. Eur. J.* **2021**, *27*, 10016–10020.
- [9] a) D. Scieszka, C. Sohr, P. Scheibenbogen, P. Marzak, J. Yun, Y. Liang, J. Fichtner, A. S. Bandarenka, *ACS Appl. Mater. Interfaces* **2018**, *10*, 21688–21695; b) D. Scieszka, J. Yun, A. S. Bandarenka, *ACS Appl. Mater. Interfaces* **2017**, *9*, 20213–20222.
- [10] a) P. Sebastián, E. Gómez, V. Climent, J. M. Feliu, *Electrochim. Acta* **2019**, *311*, 30–40; b) P. Sebastián, A. P. Sandoval, V. Climent, J. M. Feliu, *Electrochim. Commun.* **2015**, *55*, 39–42; c) V. Climent, B. A. Coles, R. G. Compton, J. M. Feliu, *J. Electroanal. Chem.* **2004**, *561*, 157–165; d) V. Climent, B. A. Coles, R. G. Compton, *J. Phys. Chem. B* **2001**, *105*, 10669–10673.
- [11] N. García-Araez, V. Climent, J. M. Feliu, *J. Phys. Chem. C* **2009**, *113*, 9290–9304.
- [12] F. J. Sarabia, P. Sebastián, V. Climent, J. M. Feliu, *J. Electroanal. Chem.* **2020**, *872*, 114068.
- [13] P. Sebastian-Pascual, F. J. Sarabia, V. Climent, J. M. Feliu, M. Escudero-Escribano, *J. Phys. Chem. C* **2020**, *124*, 23253–23259.
- [14] T. C. Nagaiah, A. Tiwari, M. Kumar, D. Scieszka, A. S. Bandarenka, *ACS Appl. Energ. Mater.* **2020**, *3*, 9, 9151–9157.
- [15] a) Q. Lenne, Y. R. Leroux, C. Lagrost, *ChemElectroChem* **2020**, *7*, 2345; b) M. Shao, Q. Chang, J.-P. Dodelet, R. Chenitz, *Chem. Rev.* **2016**, *116*, 3594–3657.
- [16] a) C. V. Rao, C. R. Cabrera, Y. Ishikawa, *J. Phys. Chem. Lett.* **2010**, *1*, 2622–2627; b) V. Colic, A. S. Bandarenka, *ACS Catal.* **2016**, *6*, 5378–5385; c) D. M. Morales, M. A. Kazakova, M. Purcel, J. Masa, W. Schuhmann, *J. Solid State Electrochem.* **2020**, *24*, 2901–2906; d) A. Alinezhad, L. Gloag, T. M. Benedetti, S. Cheong, R. F. Webster, M. Roelsgaard, B. B. Iversen, W. Schuhmann, J. J. Gooding, R. D. Tilley, *J. Am. Chem. Soc.* **2019**, *141*, 16202–16207; e) H. B. Aiyappa, J. Masa, C. Andronescu, M. Muhler, R. A. Fischer, W. Schuhmann, *Small Methods* **2019**, *3*, 1800415.
- [17] A. M. Gómez-Marín, R. Rizo, J. M. Feliu, *Catal. Sci. Technol.* **2014**, *4*, 1685–1698.
- [18] J.-C. Dong, M. Su, V. Briega-Martos, L. Li, J.-B. Le, P. Radjenovic, X.-S. Zhou, J. M. Feliu, Z.-Q. Tian, J.-F. Li, *J. Am. Chem. Soc.* **2019**, *142*, 715–719.
- [19] T. Schmidt, V. Stamenkovic, M. Arenz, N. Markovic, P. Ross Jr, *Electrochim. Acta* **2002**, *47*, 3765–3776.
- [20] a) S. Xue, R. W. Haid, R. M. Kluge, X. Ding, B. Garlyyev, J. Fichtner, S. Watzele, S. Hou, A. S. Bandarenka, *Angew. Chem. Int. Ed.* **2020**, *59*, 10934–10938; *Angew. Chem.* **2020**, *132*, 11026–11031; b) I. T. McCrum, M. T. Koper, *Nat. Energy* **2020**, *5*, 891–899; c) K. Elumeeva, J. Masa, J. Sierau, F. Tietz, M. Muhler, W. Schuhmann, *Electrochim. Acta* **2016**, *208*, 25–32.
- [21] R. Subbaraman, D. Tripkovic, D. Strmcnik, K.-C. Chang, M. Uchimura, A. P. Paulikas, V. Stamenkovic, N. M. Markovic, *Science* **2011**, *334*, 1256–1260.
- [22] N. Danilovic, R. Subbaraman, D. Strmcnik, K. C. Chang, A. Paulikas, V. Stamenkovic, N. M. Markovic, *Angew. Chem. Int. Ed.* **2012**, *51*, 12495–12498; *Angew. Chem.* **2012**, *124*, 12663–12666.
- [23] a) F. J. Sarabia, P. Sebastián-Pascual, M. T. Koper, V. Climent, J. M. Feliu, *ACS Appl. Mater. Interfaces* **2018**, *11*, 613–623; b) A. Auer, F. J. Sarabia, D. Winkler, C. Griesser, V. Climent, J. M. Feliu, J. Kunze-Liebhäuser, *ACS Catal.* **2021**, *11*, 10324–10332.
- [24] a) V. Colic, M. D. Pohl, D. Scieszka, A. S. Bandarenka, *Catal. Today* **2016**, *262*, 24–35; b) S. Xue, B. Garlyyev, S. Watzele, Y. Liang, J. Fichtner, M. D. Pohl, A. S. Bandarenka, *ChemElectroChem* **2018**, *5*, 2326–2329; c) D. Strmcnik, K. Kodama, D. van der Vliet, J. Greeley, V. R. Stamenkovic, N. Marković, *Nat. Chem.* **2009**, *1*, 466.
- [25] a) J. Zheng, W. Sheng, Z. Zhuang, B. Xu, Y. Yan, *Sci. Adv.* **2016**, *2*, e1501602; b) D. Strmcnik, P. P. Lopes, B. Genorio, V. R. Stamenkovic, N. M. Markovic, *Nano Energy* **2016**, *29*, 29–36.
- [26] P. S. Lamoureux, A. R. Singh, K. Chan, *ACS Catal.* **2019**, *9*, 6194–6201.
- [27] a) V. Climent, B. A. Coles, R. G. Compton, *J. Phys. Chem. B* **2002**, *106*, 5988–5996; b) V. Climent, B. A. Coles, R. G. Compton, *J. Phys. Chem. B* **2002**, *106*, 5258–5265.
- [28] R. Martínez-Hincapié, P. Sebastián-Pascual, V. Climent, J. M. Feliu, *Russ. J. Electrochem.* **2017**, *53*, 227–236.
- [29] A. Ganassin, P. Sebastián, V. Climent, W. Schuhmann, A. S. Bandarenka, J. M. Feliu, *Sci. Rep.* **2017**, *7*, 1246.
- [30] a) B. Garlyyev, S. Xue, S. Watzele, D. Scieszka, A. S. Bandarenka, *J. Phys. Chem. Lett.* **2018**, *9*, 1927–1930; b) S. Xue, B. Garlyyev, A. Auer, J. Kunze-Liebhäuser, A. S. Bandarenka, *J. Phys. Chem. C* **2020**, *124*, 12442–12447; c) B. Garlyyev, S. Xue, M. D. Pohl, D. Reinisch, A. S. Bandarenka, *ACS*

- Omega* **2018**, *3*, 15325–15331; d) V. Briega-Martos, F. J. Sarabia, V. Climent, E. Herrero, J. M. Feliu, *ACS Meas. Sci. Au* **2021**, 10.1021/acsmesuresciau.1c00004.
- [31] A. Rabis, P. Rodriguez, T. J. Schmidt, *ACS Catal.* **2012**, *2*, 864.
- [32] R. M. Dell, *Solid State Ionics* **2000**, *134*, 139.
- [33] S. Pratihar, A. Chandra, *J. Chem. Phys.* **2011**, *134*, 024519.
- [34] a) W. Li, S. Xue, S. Watzele, S. Hou, J. Fichtner, A. L. Semrau, L. Zhou, A. Welle, A. S. Bandarenka, R. A. Fischer, *Angew. Chem. Int. Ed.* **2020**, *59*, 5837–5843; *Angew. Chem.* **2020**, *132*, 5886–5892; b) W. Li, S. Watzele, H. A. El-Sayed, Y. Liang, G. Kieslich, A. S. Bandarenka, K. Rodewald, B. Rieger, R. A. Fischer, *J. Am. Chem. Soc.* **2019**, *141*, 5926–5933; c) S. Hou, W. Li, S. Watzele, R. M. Kluge, S. Xue, S. Yin, X. Jiang, M. Döblinger, A. Welle, B. Garlyyev, P. Müller-Buschbaum, C. Wöll, A. S. Bandarenka, R. A. Fischer, *Adv. Mater.* **2021**, 10.1002/adma.202103218.

Manuscript received: August 31, 2021

Revised manuscript received: December 9, 2021

Accepted manuscript online: December 15, 2021